Supplementary material: additional heat paper

Luke Fraser-Leach, Paul Kushner, Alexandre Audette

October 3, 2023

1 Stability of the EBM to sea ice perturbations

Consider an EBM state perturbed from a stable equilibrium solution (main text equation 2, M2). The annual mean global mean tendency of the surface enthalpy perturbation is obtained by taking the annual and global mean of (1) minus (2).

$$\frac{\partial \delta\langle\overline{E}\rangle}{\partial t} = \delta\langle\overline{aS}\rangle - B\delta\langle\overline{T}\rangle \tag{1}$$

Here, δ symbols denote perturbations from equilibrium, i.e. differences in the state variables between (M1) and (M2). Assuming $\delta\langle\overline{aS}\rangle \approx \left(\partial\langle\overline{aS}\rangle/\partial\langle\overline{T}\rangle\right)\delta\langle\overline{T}\rangle$, where the partial derivative represents the expected increase of coalbedo with temperature for a given spatial pattern of forcing (in this case F_{ghg}), this becomes

$$\frac{\partial \delta\langle\overline{E}\rangle}{\partial t} \approx -\delta\langle\overline{T}\rangle \left(B - \frac{\partial\langle\overline{aS}\rangle}{\partial\langle\overline{T}\rangle} \right). \tag{2}$$

For the equilibrium to be stable, $\partial\delta\langle\overline{E}\rangle/\partial t$ must be of opposite sign to $\delta\langle\overline{E}\rangle$. E is a piecewise function of T, so it does not clarify things to write equation (2) only in terms of T. In the absence of sea ice, E is a positive linear function of T, but in the presence of sea ice the relationship is complex (Wagner & Eisenman, 2015). Most regions are ice-free for most of the year, so it is reasonable to assume that $\langle\overline{E}\rangle$ is a monotonically increasing function of $\langle\overline{T}\rangle$. Under this assumption, $\partial\delta\langle\overline{E}\rangle/\partial t$ has the same sign as $\partial\langle\overline{E}\rangle/\partial t$, both of which must be of opposite sign to $\delta\langle\overline{T}\rangle$ for a stable equilibrium. Clearly, this is only true if

$$B > \frac{\partial\langle\overline{aS}\rangle}{\partial\langle\overline{T}\rangle}. \tag{3}$$

In other words, sea ice perturbations cannot be self sustaining in a stable climate.

2 Pattern scaling calculation

Blackport and Kushner (2017) show that for a simulation representing a future warmed climate with LLW $\delta T_{l,ghg}$ and SIL δI_{ghg}, and a sea ice perturbation simulation with LLW $\delta T_{l,pert}$ and SIL δI_{pert}, the sensitivities of some field Z to these two parameters are given by

$$
\begin{pmatrix} \left.\frac{\partial Z}{\partial T_l}\right|_I \\ \left.\frac{\partial Z}{\partial I}\right|_{T_l} \end{pmatrix} = \frac{1}{\delta I_{pert}\delta T_{l,ghg} - \delta I_{ghg}\delta T_{l,pert}} \begin{pmatrix} -\delta I_{ghg} & \delta I_{pert} \\ \delta T_{l,ghg} & -\delta T_{l,pert} \end{pmatrix} \cdot \begin{pmatrix} \delta Z_{pert} \\ \delta Z_{ghg} \end{pmatrix}.
\tag{4}
$$

Considering the EBM, the partial temperature response to LLW is

$$
\frac{\partial T}{\partial T_l} = \frac{\delta I_{pert}\delta T_{ghg} - \delta I_{ghg}\delta T_{pert}}{\delta I_{pert}\delta T_{l,ghg} - \delta I_{ghg}\delta T_{l,pert}}
\tag{5}
$$

Assuming the sea ice perturbation method accurately achieves the target, $\delta I_{pert} = \delta I_{ghg}$ and $\delta(aS)_{pert} = \delta(aS)_{ghg}$. We also assume that there is little LLW in the sea ice perturbation simulation, i.e. $\delta T_{l,pert} \ll \delta T_{l,ghg}$, to simplify the denominator. This gives

$$
\frac{\partial T}{\partial T_l} \approx \frac{\delta T_{ghg} - \delta T_{pert}}{\delta T_{l,ghg} - \delta T_{l,pert}}
\tag{6}
$$

From equation (2), the global mean annual temperature response in the FUTURE EBM simulation is

$$
\delta\langle\overline{T}\rangle_{ghg} = B^{-1}\left(\delta\langle\overline{aS}\rangle_{ghg} + F_{ghg}\right),
\tag{7}
$$

and the temperature response in the perturbation simulation is

$$
\delta\langle\overline{T}\rangle_{pert} = B^{-1}\left(\delta\langle\overline{aS}\rangle_{ghg} + \langle\overline{F_{pert}}\rangle\right),
\tag{8}
$$

where F_{pert} is the artificial heat flux in any of the perturbation methods. Taking the global and

2

annual mean of (6) and substituting these expressions, we obtain

$$\frac{\partial \langle \overline{T} \rangle}{\partial T_l} \approx \frac{B^{-1}\left(F_{ghg} - \langle \overline{F_{pert}} \rangle\right)}{\delta T_{l,ghg}}. \tag{9}$$

$\partial T/\partial I$ is obtained by the same procedure. Assuming $\delta I_{pert} = \delta I_{ghg} \equiv \delta I$ yields

$$\frac{\partial T}{\partial I} = \frac{\delta T_{l,ghg}\delta T_{pert} - \delta T_{l,pert}\delta T_{ghg}}{\delta I(\delta T_{l,ghg} - \delta T_{l,pert})}. \tag{10}$$

Assuming little LLW in the perturbation simulation, taking the global mean, and substituting equations (7) and (8) gives

$$\frac{\partial \langle \overline{T} \rangle}{\partial I} \approx \frac{1}{B}\frac{\delta \langle \overline{aS} \rangle_{ghg} + \delta \langle \overline{F_{pert}} \rangle - \left(\delta \langle \overline{aS} \rangle_{ghg} + F_{ghg}\right)\left(\delta T_{l,pert}/\delta T_{l,ghg}\right)}{\delta I \left(1 - \delta T_{l,pert}/\delta T_{l,ghg}\right)}. \tag{11}$$

Assuming $\delta T_{lpert} \ll \delta T_{lghg}$, this becomes

$$\frac{\partial \langle \overline{T} \rangle}{\partial I} \approx \frac{B^{-1}\left(\delta \langle \overline{aS} \rangle_{ghg} + \delta \langle \overline{F_{pert}} \rangle\right)}{\delta I}. \tag{12}$$

We obtain the EBM sensitivities to the new parameters F_{ice} and F_{ghg} the same way, except that the only assumption required to obtain the expressions in the text is that the perturbation simulation accurately achieves the target sea ice state, so that $\delta(aS)_{pert} = \delta(aS)_{ghg}$.
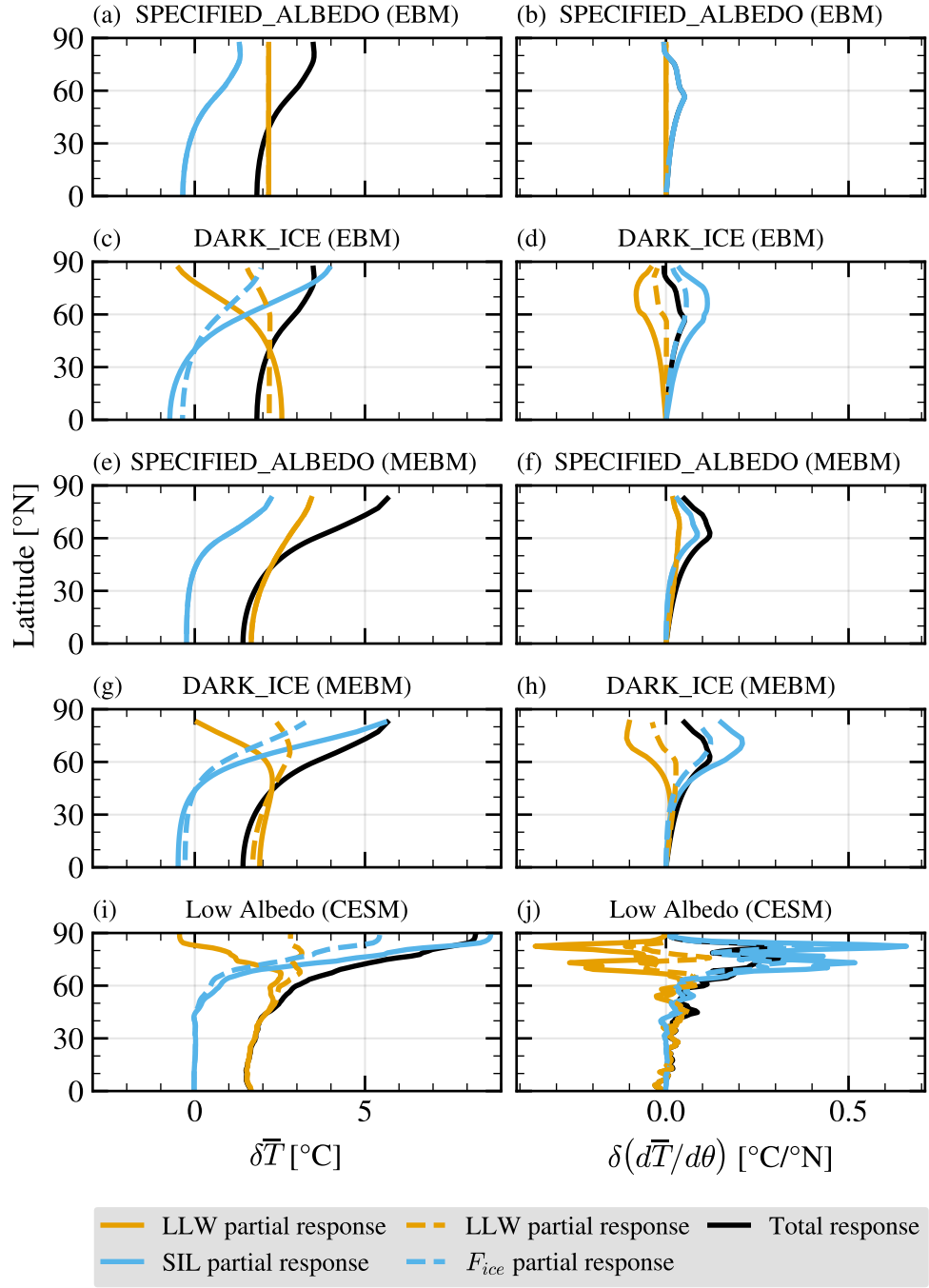
3   LLW vs. F_{ghg} as a scaling parameter

Figure S1: As in Figure 2, but dashed gold and blue curves show the partial responses to LLW and F_{ice} (as opposed to F_{ghg} and F_{ice}), respectively. The main difference between the two sets of plots is a global mean offset in the dashed curves, which has no bearing on our conclusions.

4 Accounting for additional heat in nudging simulations

In addition to the modified albedo simulations, we repeated our analysis on nudging simulations in the EBMs and in CESM. In this case, we define F_{ice} differently from the albedo modification case. In nudging simulations, we cannot define F_{ice} as the simple change in net TOA shortwave - this would only reflect physical changes in albedo and would not capture the artificial heat added by nudging. Instead, we add the nudging heat flux to the TOA shortwave change, giving $F_{ice} = S\delta a + F_{nudge}$. In the hybrid nudging scheme (Audette & Kushner, 2022), $F_{nudge} = \delta F_{hyb} + L_f h_{thin} \delta SIC$, where F_{hyb} is the heat flux applied to all categories of sea ice in each grid cell, L_f is the latent heat of fusion of seawater, and h_{thin} is the mean thickness of the thinnest category of sea ice in each grid cell. Using this parameter to account for the additional heat is not as clean as our definition of F_{ice} in albedo modification simulations, because $S\delta a$ and F_{nudge} represent different processes. In comprehensive models, the nudging flux is seen only by the sea ice model, while the net TOA shortwave directly affects the entire atmospheric column and the surface. This is in contrast to $F_{ice} = S\delta a$ in albedo modification simulations, where we used the change in TOA shortwave to capture both the shortwave forcing from the physical albedo feedback and from artificial darkening of the ice, both of which are seen by the whole model.

Nonetheless, using F_{ice} as a scaling parameter successfully accounts for the artificial heat in the EBMs (top four rows of figure S2). This is because the EBM is too simple for a nudging flux to be applied only to the sea ice component, so the nudging flux directly affects the surface energy balance, and the above-mentioned caveat does not apply in this model. In contrast, scaling by F_{ice} in the WACCM hybrid nudging simulations does not properly account for the artificial heat (bottom row of figure S2). The new scaling parameter attributes nearly the entire surface temperature response to LLW, and almost no warming to SIL. This feature is also present in the air temperature and zonal wind fields (not shown).

Examining the F_{nudge} and $S\delta a$ fields in the hybrid nudging simulations reveals that they should not be added on an equal footing. Figure S3 shows that the total nudging flux from 70-90°N in pafutArcSIC is more than twice the total change in TOA shortwave integrated over the same region, so that artificial heat accounts for about 70% of F_{ice}. By comparison, we estimate that artificial heat accounts for about 30% of F_{ice} in Low Albedo. One interpretation of this large nudging flux is that
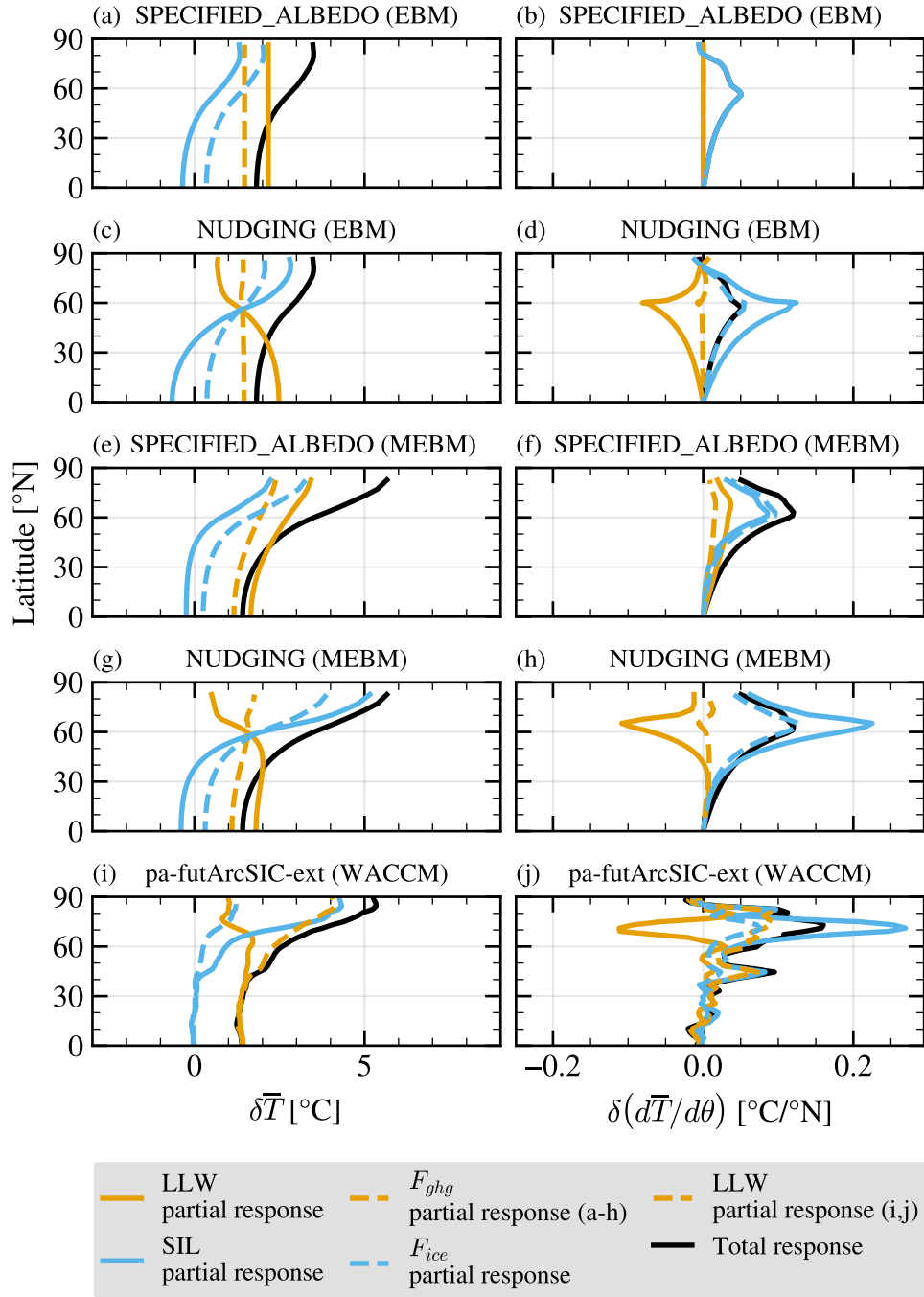
Figure S2: As in Figure 3, but for the nudging simulations in the EBM (top four rows) and the CESM-WACCM hybrid nudging simulations (bottom row).
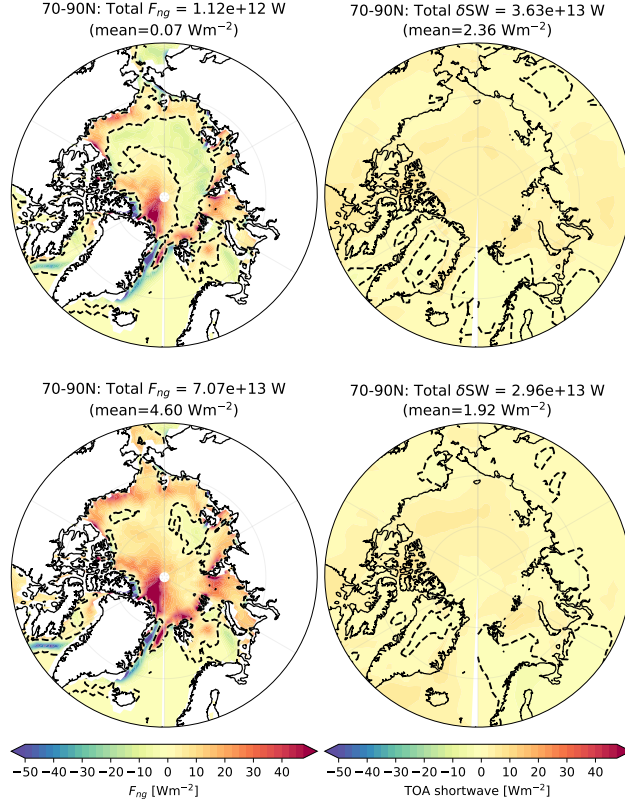
Figure S3: The heat flux added by the hybrid nudging method (a) compared to the change in net TOA shortwave (b). Both quantities are differences from the pa-pdSIC control simulation (a nonzero nudging flux is added in that simulation to achieve the desired control ice conditions). In the hybrid nudging method, F_{nudge} is the sum of a heat flux added to the bottom of the sea ice and implicit latent heat added by directly converting thinnest category ice to freshwater (Audette & Kushner, 2022).

the artificial heat added by the nudging method is inducing a huge spurious response, responsible for almost the entire climate response according to pattern scaling (figure S2). This is unlikely, given that nudging methods give similar climate responses to the albedo modification method (Sun et al., 2020). Rather, it seems that we have not chosen the correct scaling parameter for the nudging method. Because it is only seen by the sea ice model, a unit of nudging flux probably does not have as great an influence on the climate system as a unit change in net TOA shortwave.

A more accurate choice of F_{ice} in ghost flux simulations would quantify the effect of the F_{pert} on the surface energy budget. Shaw and Smith (2022) analyzed the effect of sea ice loss on the surface energy budget using slab ocean simulations with no sea ice and fully coupled sea ice perturbation simulations. They find that in non-perturbation simulations, the change in turbulent heat flux due to sea ice loss is a response to the increase in absorbed shortwave, as expected. However, in the sea
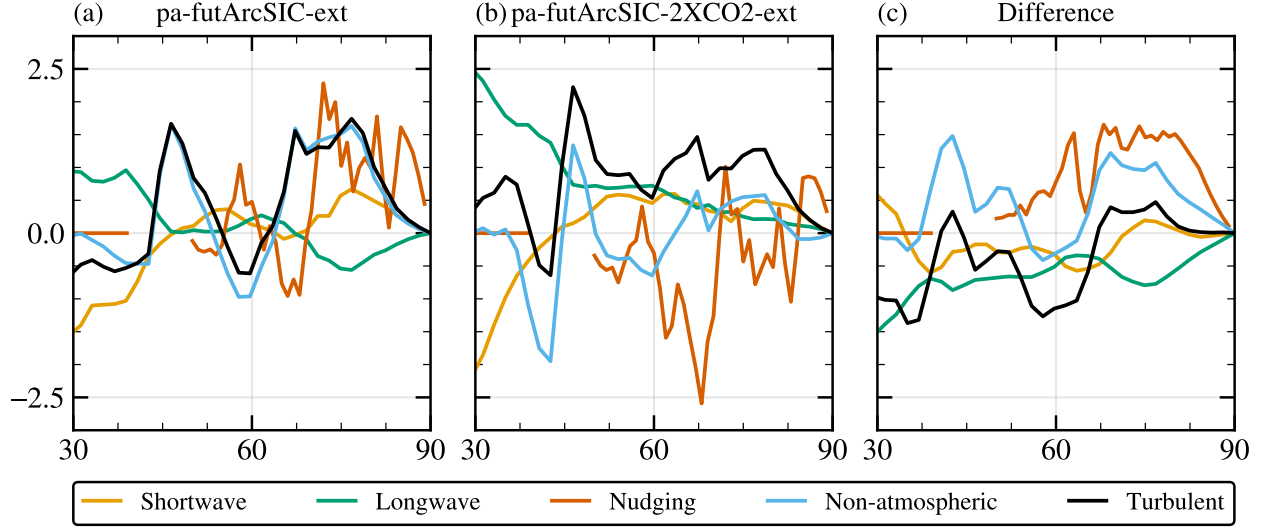
Figure S4: Annual mean zonal mean cosine-weighted surface energy fluxes for (a) pa-futArcSIC-ext relative to pa-pdSIC-ext, (b) pa-futArcSIC-2XCO2-ext relative to pa-pdSIC-ext, and (c) pa-futArcSIC-ext relative to pa-futArcSIC-2XCO2-ext. Positive is defined as into the ocean column, except for the turbulent flux. The non-atmospheric flux is calculated as the change in total surface heat flux.

ice perturbation simulations, the change in turbulent heat flux largely balances the heat flux into the ocean column due to ocean and sea ice processes (the non-atmospheric flux, F_{na}). We find the same effect in the CESM-WACCM hybrid nudging experiments figure S5. This suggests that F_{na} may quantify the effect of artificial heat on the surface energy budget. The spatial pattern of F_{na} shows some similarity to the nudging flux, but is generally smoother and reduced in magnitude. In particular, the difference in the fluxes between pa-futArc-2XCO2-ext and pa-futArc-ext show and F_{na} which generally resembles the nudging flux in spatial structure but is reduced in magnitude (figure S5c). However, there are significant differences in the spatial structure of the changes to the two fluxes in the nudging simulations, for example in the Arctic Ocean off the north coast of Greenland (not shown). Another option is to use the turbulent heat flux as F_{ice}, as it mainly balances the sum of the changes to the non-atmospheric and absorbed shortwave fluxes, and may best quantify the effect of sea ice changes on the lower atmosphere. The sign of the turbulent heat flux has been used to diagnose artificial effects of SST nudging experiments (O'Reilly et al., 2023). More rigorous justification of the use of either of these as F_{pert} would require an EBM with separate atmosphere and ocean layers and a representation of the energy fluxes between them.

   The surface temperature partial responses to these two new variables are shown in figure S4.
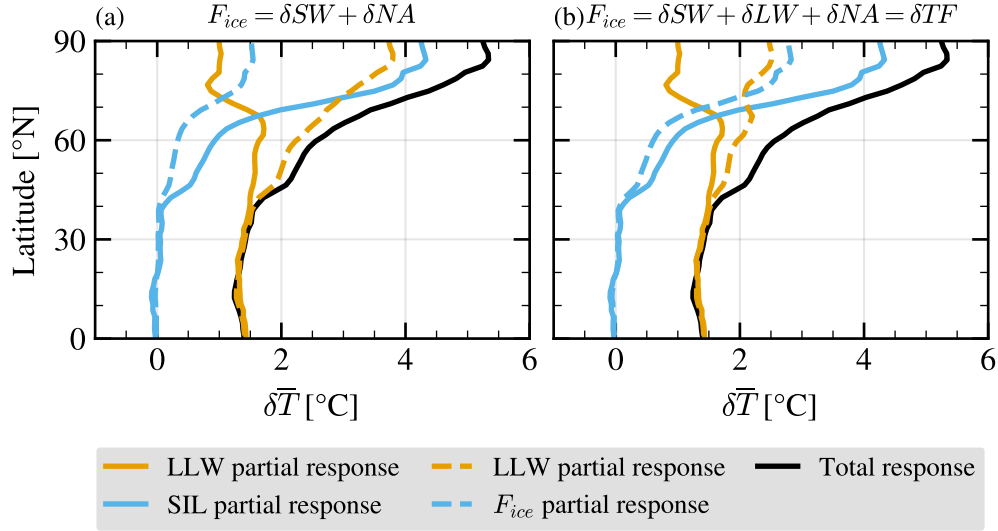
Figure S5: As in Figure 3, but with F_ice equal to (a) the change in shortwave plus the change in non-atmospheric flux and (b) the change in surface turbulent heat flux.

Using the non-atmospheric flux as F_{pert} yields a similar (though slightly less dramatic) result as using the nudging flux: F_{pert} dominates the change in shortwave so that most of the response is attributed to LLW figure S4a. However, the difference in Arctic longwave fluxes is significant between the pa-futArcSIC-ext and pa-futArcSIC-2XCO2 (as it is in the ghost flux simulations analyzed in Shaw and Smith (2022)), suggesting it may be important to add it to the shortwave response. Doing this is equivalent to setting F_{pert} equal to the change in surface turbulent heat flux, since F_{na} is calculated as a residual. Using the turbulent heat flux does give surface temperature partial responses more similar to the EBM (figure S4b), but we do not pretend that this choice has been rigorously justified.